Risk-Constrained Coordination of Cascaded Hydro Units With Variable Wind Power Generation

Lisias V. L. Abreu, *Member, IEEE*, Mohammad E. Khodayar, *Student Member, IEEE*, Mohammad Shahidehpour, *Fellow, IEEE*, and Lei Wu, *Member, IEEE*

***Abstract*—This paper presents a stochastic hourly coordination strategy for wind units and cascaded hydro generation as storage to firm up the hourly dispatch in a generating company (GENCO). The proposed strategy is based on the stochastic price-based unit commitment (Stochastic PBUC) formulation which includes wind energy imbalance charges. The forecast errors of electricity market price and wind speed are simulated with the Monte Carlo method via a scenario approach. The risk-aversion constraints are considered for limiting a GENCO's financial risks when considering uncertain wind power generation. The proposed optimization model is solved by mixed-integer linear programming (MIP) and illustrative examples examine the effectiveness of the proposed risk-based coordination model for optimizing a GENCO's payoff.**

***Index Terms*—Cascaded hydro and wind coordination, risk-aversion, stochastic price-based unit commitment.**

NOMENCLATURE

Variables:

EDR	Expected downside risk ($).
h, h'	Denote a cascaded hydro unit.
I_{ht}	Commitment status of hydro unit h at hour t.
k	Denote an intrahour interval.
$P_{C,ht}$	Coordinated generation dispatch corresponding to hydro unit h at hour t (MW).
PF^s	Payoff of scenario s ($).
P_{ht}	Dispatch of hydro unit h at hour t (MW).
P^s_{htk}	Dispatch of hydro unit h at hour t and intrahour interval k in scenario s (MW).
P_{wt}	Dispatch of wind unit w at hour t (MW).
P^s_{wtk}	Dispatch of wind unit w at hour t and intrahour k in scenario s (MW).
$P^{c,s}_{wtk}$	Curtailed wind power of wind unit w at hour t and intrahour interval k in scenario s (MW).
$P^s_{\Delta,wtk}$	Imbalance power of wind unit w at hour t and intrahour interval k in scenario s (MW).
$P^s_{\lvert\Delta\rvert,wtk}$	Absolute imbalance power of unit w at hour t and intrahour interval k in scenario s (MW).
q_{ht}	Water discharge of hydro unit h at hour t (Hm^3/h).
q^s_{htk}	Discharge of hydro unit h at hour t and intrahour interval k in scenario s (Hm^3/h).
$q_{d,h(t-\tau)}$	Discharge to hydro unit h from upstream hydro units with the delay time τ at time t (Hm^3/h).
R^s	Downside risk of scenario s ($).
r_{ht}	Natural inflow of hydro unit h at hour t (Hm^3/h).
s	Denote a scenario.
s_{ht}	Spillage of hydro unit h at hour t in scenario s (Hm^3/h).
t	Hour index.
v_{ht}	Reservoir volume of hydro unit h at hour t (Hm^3).
v^s_{ht}	Reservoir volume of hydro unit h at hour t in scenario s (Hm^3).
w	Denote a wind unit.
y_{ht}, z_{ht}	Operation status/shutdown indicator of hydro unit h at hour t.
$\delta^s_{\Delta,wtk}, \delta^s$	Auxiliary binary variables.

Constants:

$\overline{\text{EDR}}$	Targeted expected downside risk target ($).
$F_h(\,)$	Water-to-power conversion curve of hydro unit h.
NK	Number of intrahour intervals.
NH	Number of hydro units.
NS	Number of scenarios.
p^s	Probability of scenario s.
$P^{\min}_h, P^{\max}_h$	Min/Max generation of hydro unit h.

Manuscript received July 14, 2011; revised December 08, 2011; accepted January 12, 2012. Date of publication May 01, 2012; date of current version June 15, 2012. This work was supported in part by the NSF Grant ECCS-0801853 and in part by the U.S. Department of Energy Grant DE-EE 0002979 and Grant DE-EE 0001380.000.

L. V. L. Abreu, M. E. Khodayar, and M. Shahidehpour are with the Electrical and Computer Engineering Department, Illinois Institute of Technology, Chicago, IL 60616 USA (e-mail: lisias@ieee.org; mkhodaya@iit.edu; ms@iit.edu).

L. Wu is with the Electrical and Computer Engineering Department, Clarkson University, Potsdam, NY 13699 USA (e-mail: lwu@clarkson.edu).

Digital Object Identifier 10.1109/TSTE.2012.2186322

$P_{wtk}^{f,s}$	Forecasted wind power of unit w at hour t and intrahour interval k in scenario s (MW).
P_{wt}^{f}	Forecasted wind power unit w at hour t (MW).
$q_h^{\min}, q_h^{\max}$	Min/Max discharge limits of hydro unit h(Hm^3/h).
RC_h	Geographic reservoir connection vector of hydro unit h.
$rc_{h-h'}$	Binary variable representing the direct cascaded configuration of hydro units h and h'.
$\mathrm{RU}_h, \mathrm{RD}_h$	Ramp up/down limits of hydro unit h (MW/min).
$\mathrm{SU}_h, \mathrm{SD}_h$	Startup/shutdown cost of hydro unit h(\$).
$S_{C,h}$	Set of wind units in coordination with hydro unit h.
$s_h^{\min}, s_h^{\max}$	Min/Max spillage limits of hydro unit h(Hm^3/h).
T_0	Target payoff of a GENCO (\$).
$V_h^{\min}, V_h^{\max}$	Min/Max reservoir volume limits of hydro unit h(Hm^3).
$V_{0,h}, V_{NT,h}$	Initial/terminal water reservoir of hydro unit h(Hm^3).
$X(t)$	Wind forecast error at time t.
$Z(t)$	Random Gaussian variable with the mean equal to zero and corresponding standard deviation.
α, β	ARMA constants.
ρ_{BP}^{s}	Energy balancing price in scenario s (\$/MWh).
$\rho_{\mathrm{DA},t}^{s}$	Day-ahead energy market price at hour t in scenario s (\$/MWh).
$\rho_{\mathrm{RT},tk}^{s}$	Real-time market price at hour t and intrahour interval k in scenario s (\$/MWh).

I. Introduction

A GENCO's objective is to maximize profit through market participation. Price-based unit commitment (PBUC) is a decision tool that is used by GENCOs for procuring the optimal generation bids and/or self-scheduling decisions in day-ahead by considering market price forecasts. However, GENCOs, as market participants, have no obligation to balance supply with loads. Independent system operators (ISOs) use a security-constrained unit commitment (SCUC) tool that would utilize the submitted bids to clear the day-ahead market. ISOs balance supply with loads in a secure and economic fashion.

Usually, the perfect information on the day-ahead market price and wind speed is not available. Thus, GENCOs apply a stochastic model for forecasting hourly wind speed and market price. A stochastic PBUC model is then utilized that would maximize the GENCO's payoff while minimizing its financial risks. The GENCO's payoff consists of energy sales minus the cost of energy production and imbalance penalties. The cost of imbalance energy could reduce the GENCO's potential payoff if the real-time energy dispatch does not match that of day ahead.

The GENCO's finances may be subject to major risks when considering wind energy forecast errors. In general, the daily pattern for wind energy may not coincide with that of electricity demand. Wind energy imbalance charges may be incurred if the real-time wind energy differs from the day-ahead schedule [1]–[10]. The lack of dispatchability of installed wind energy capacity would make it difficult for GENCOs to take advantage of daily differences in electricity prices.

The wind energy forecast errors could also have a major impact on the secure operation of power systems. The ISO may consider preventive and corrective actions for managing the secure operation of power systems with intermittent and volatile wind energy [11]. A stochastic model was applied in [12] to examine the impact of high penetration of wind energy on power system operations. The auto-regressive moving average (ARMA) time series model was considered in [13] to simulate the wind speed volatility. A deterministic PBUC was applied for developing fossil unit bidding strategies [14]–[16]. A stochastic PBUC solution was presented in [17] and [18] for formulating power market dynamics.

This paper proposes a risk-constrained day-ahead coordination strategy for wind and cascaded hydro (storage) units in a GENCO. Wind energy variations could occur within minutes while the day-ahead schedule is hourly, so an intrahour-based model is proposed in this paper to firm up the coordinated wind and hydro generation. The paper shows that the fast ramping and storage capabilities of cascaded hydro units could compensate wind energy volatilities. The Monte Carlo simulation is used to generate scenarios, and scenario reduction techniques are applied to eliminate low-probability scenarios and bundle similar ones to identify a limited number of effective scenarios while maintaining a reasonably good approximation of the original system [19]. The advantage of applying the Monte Carlo simulation resides in the fact that the required number of samples for a given accuracy level is independent of the system uncertainty dimension, and, therefore, is suitable for the simulation of power systems with a large number of uncertainties.

Scenario reduction algorithms include the fast backward method, the fast backward/forward method, and the fast backward/backward method [19], [20]. The algorithms have different computational performance, and the choice of algorithms for a certain problem depends on the size of the problem and the required solution accuracy. For large scenario trees, the fast backward method would provide the best computational performance with the worst accuracy. The results of the fast forward method are more accurate at the cost of longer computational time. In this paper, the fast backward/forward method is selected to reduce the number of scenarios.

The day-ahead hourly market clearing prices (MCPs) are provided as input and the uncertainty of MCPs is represented via scenarios using time series [17], [18]. There is no transmission congestion considered between wind and hydro unit locations

(i.e., day-ahead hourly prices are the same for wind and hydro units.) The real-time energy balancing prices are announced daily by the ISO [21]. The energy balancing cost is the daily cost of deviation in the real-time dispatch of market entities, which is allocated as credit to other generating units for supplying energy deviations, or as credit to real-time system demand for enhancing the system reliability.

The rest of the paper is organized as follows. Section II provides the stochastic PBUC formulation with the wind-hydro intrahour coordination. Section III illustrates the proposed formulation in two examples, and the conclusion is presented in Section IV.

II. Stochastic PBUC Formulation

The objective of PBUC is to maximize a GENCO's payoff, which is the revenue from the sales of energy or bilateral contracts minus the operation cost of GENCO. The operation cost includes the production cost, startup/shut down costs, and imbalance energy charges incurred by wind energy variations. In this paper, we focus on the coordination strategy of wind and hydro units, thus the hourly scheduling of other types of generating units (thermal, combined-cycle, and pumped-storage units) is not discussed [17], [18].

In the proposed stochastic PBUC problem, there are first- and second-stage variables. A first-stage variable is stated as a decision variable which is made before uncertainties are disclosed, that is, yielding identical values in all scenarios such as $P_{C,ht}$. A second-stage variable is scenario-dependent, which can be an intrahour variable depending on t, k, and s such as $P^s_{\Delta,wtk}$. The stochastic PBUC formulation is discussed next for the wind-hydro coordination.

A. Uncoordinated Scheduling of Wind and Hydro Units

The stochastic PBUC would maximize the GENCO's expected payoff (1), subject to prevailing constraints. The first term in the objective function is the revenue from hydro and wind energy sales to day-ahead markets. The second term represents the operation cost of hydro units which includes startup and shutdown costs. The imbalance charges for wind units included in the last two terms of (1) are $P^s_{\Delta,wtk}$ paid based on $\rho^s_{RT,tk}$ and $P^s_{|\Delta|,wtk}$ paid based on ρ^s_{BP}.

Since the coordinated scheduling of cascaded hydro and wind units is not considered here, the objective function of hydro-wind can be decoupled into two independent optimization problems. The water to power curve of hydro unit h, expressed in (2) is generally a nonlinear, nonconvex curve [22], in which the hydro power generation has a nonlinear correlation with the water flow through the turbine and water head. Using auxiliary binary variables, the nonconvex water to power curve can be converted into the piecewise linearized model and incorporated into the proposed MIP formulation [18], [22], [23]. There are two popular methods used in the power industry for solving such MIP models including the branch-and-bound/branch-and-cut and Lagrangian Relaxation [24]. The advantages of branch-and-bound/branch-and-cut over the Lagrangian Relaxation approach for solving the MIP-based PBUC problem was discussed in detail in [25]. It was shown that the branch-and-bound/branch-and-cut-based method would

$$\begin{aligned}
&\text{maximize} \quad \sum_{s=1}^{\mathrm{NS}} p^s \cdot PF^s \\
&= \sum_{s=1}^{\mathrm{NS}} p^s \cdot \left[\begin{array}{l} \displaystyle\sum_h \sum_t \rho^s_{\mathsf{DA},t} \cdot P_{ht} + \sum_w \sum_t \rho^s_{\mathsf{DA},t} \cdot P_{wt} - \sum_h \sum_t \left(y_{ht} \cdot SU_h + z_{ht} \cdot SD_h\right) \\ \displaystyle -\sum_w \sum_t \left(\tfrac{1}{NK} \cdot \sum_k \rho^s_{\mathsf{RT},tk} \cdot P^s_{\Delta,wtk} + \tfrac{1}{NK} \cdot \rho^s_{\mathsf{BP}} \cdot \sum_k P^s_{|\Delta|,wtk} \right) \end{array} \right] \qquad (1) \\
&P_{ht} = F_h(q_{ht}) \qquad (2) \\
&q_h^{\min} \cdot I_{ht} \le q_{ht} \le q_h^{\max} \cdot I_{ht} \qquad (3) \\
&V_h^{\min} \le v_{ht} \le V_h^{\max} \qquad (4) \\
&v_{h(0)} = V_{0,h}, v_{h(NT)} = V_{NT,h} \qquad (5) \\
&v_{h(t+1)} = v_{ht} + RC_h \cdot q_{d,h(t-\tau)} - q_{ht} + r_{ht} - s_{ht} \qquad (6) \\
&s_h^{\min} \le s_{ht} \le s_h^{\max} \qquad (7) \\
&q_{d,h(t-\tau)} = \left[q_{1(t-\tau)} \cdots q_{(h-1)(t-\tau)}\ 0\ q_{(h+1)(t-\tau)} \cdots q_{NH(t-\tau)}\right] \qquad (8) \\
&P_{wt} = P^s_{wtk} + P^s_{\Delta,wtk} \qquad (9) \\
&0 \le P_{wt} \le P^f_{wt} \qquad (10) \\
&0 \le P^s_{wtk} \le P^{f,s}_{wtk} \qquad (11) \\
&P^s_{|\Delta|,wtk} - P^s_{\Delta,wtk} \ge 0 \qquad (12) \\
&P^s_{|\Delta|,wtk} + P^s_{\Delta,wtk} \ge 0 \qquad (13) \\
&P^s_{|\Delta|,wtk} - P^s_{\Delta,wtk} \le M \cdot \delta^s_{\Delta,wtk} \qquad (14) \\
&P^s_{|\Delta|,wtk} + P^s_{\Delta,wtk} \le M \cdot \left[1 - \delta^s_{\Delta,wtk}\right] \qquad (15)
\end{aligned}$$

procure a near-optimal/good-enough solution with enhanced modeling and convergence acceleration strategies.

Other constraints include water discharge limits (3), reservoir volume (4), initial and terminal reservoir volume (5), water balance constraints for cascaded hydro units (6), and water spillage limits (7). Minimum on/off time and ramping up/down constraints are given in [17] and [18]. In (6), RC_h is the geographic reservoir connection vector with binary elements $rc_{h-h'}, rc_{h-h'} = 1$ if the hydro unit h' is a direct up stream of unit h; otherwise $rc_{h-h'} = 0$. In addition, $q^s_{d,h(t-\tau)}$ in (8) represents the delayed water discharge to the hydro unit h from upstream hydro units.

Since wind speed variations could occur within minutes, the intrahour variations of wind generation is integrated into the proposed scheduling model. In this paper, the wind speed forecast is procured by the Markov chain with the probability transition matrix. Wind speed values are classified into several categories represented by the mean value at each group. The probability transition matrix can either be obtained by historical data or by probability distribution parameters of the wind speed. Using the Weibull distribution function and the autocorrelation factor, the probability transition matrix is procured by composing an initial probability vector, a weighting matrix and a normalizing vector [26]. The probability transition matrix, which is a square matrix, defines probabilities of transiting from one wind speed category to other wind speed categories. Once the probability transition matrix is built, the wind speed time series can be procured with the Markov chain method. The wind speed forecast error is further represented by ARMA [27], [28]. Since the number of time steps for one day is not large enough (144 time steps for one day considering 10-min interval), the synthesized time series may have mean and standard deviations that are different from the corresponding values in the Weibull distribution function. Thus, the mean and the standard deviation are adjusted to procure the desired wind speed time series. The diurnal pattern strength which represents the daily pattern of wind speed is applied to the time series. The diurnal pattern has the sinusoidal form, in which the peak value indicates the ratio of the maximum wind speed to the average wind speed. The intrahour-based wind unit constraints include hourly and intrahour power generation schedule (9) and generation limits (10)–(11). The available wind energy is calculated using the wind speed forecast and used as input to PBUC. Equations (12)–(15) incorporate $P^s_{|\Delta|,wtk}$ in the stochastic PBUC problem, where M is a large positive number.

B. Coordinated Scheduling of Wind and Hydro Units

In this case, the coordinated scheduling of cascaded hydro unit with one or more wind units is considered for providing an hourly firm power dispatch. The first term in (16) shows the GENCO's revenue and the second term represents the operation cost of hydro unit. Since the hourly wind generation is firm, the imbalance energy charge will be zero. The unit commitment (UC) of hydro and wind units determines the hourly on/off status, and the generation dispatch provides a 10-min solution. Thus, by coordination, the sum of intrahour wind P^s_{wtk} and hydro P^s_{htk} generation is equal to the hourly generation dispatch $P_{C,ht}$ (17). Note that $P_{C,ht}$ is a scenario-independent first-stage decision variable, which is calculated before uncertainties are imposed. The wind power (P^f_{wtk}) is dependent on the wind speed forecast. The wind power generation follows the power curve of the wind turbine, which is zero below the cut-in or above the cut-out speeds.

$$\begin{aligned}\text{maximize} \quad & \sum_{s=1}^{\text{NS}} p^s \cdot \text{PF}^s \\ &= \sum_{s=1}^{\text{NS}} p^s \cdot \left[\sum_h \sum_t \rho^s_{\text{DA},t} \cdot P_{C,ht} \right. \\ &\qquad \left. - \sum_h \sum_t (y_{ht} \cdot SU_h + z_{ht} \cdot SD_h) \right] \end{aligned} \tag{16}$$

$$P_{C,ht} = \sum_{w \in S_{C,h}} P^s_{wtk} + P^s_{htk} \tag{17}$$

$$P^s_{wtk} = P^{s,f}_{wtk} - P^{c,s}_{wtk} \quad \forall w, \forall t, \forall k, \forall s \tag{18}$$

$$q^{\min}_h \cdot I_{ht} \le q^s_{htk} \le q^{\max}_h \cdot I_{ht} \tag{19}$$

$$\begin{aligned} &P^s_{ht(k+1)} - P^s_{htk} \le 60 \cdot RU_h/NK \\ &P^s_{htk} - P^s_{ht(k+1)} \le 60 \cdot RD_h/NK \end{aligned} \tag{20}$$

$$I_{ht} - I_{h(t-1)} = z_{ht} - y_{ht} \tag{21}$$

$$z_{ht} + y_{ht} \le 1 \tag{22}$$

$$P^s_{htk} = F_h\left(q^s_{htk}\right) \tag{23}$$

$$V^{\min}_h \le v^s_{htk} \le V^{\max}_h \tag{24}$$

$$v^s_{h(0)NK} = V_{0,h}, \quad v^s_{h(NT)NK} = V_{NT,h} \tag{25}$$

$$\begin{aligned} v^s_{htk} &= v^s_{ht(k-1)} + \frac{1}{NK} \\ &\quad \cdot \left(RC_h \cdot q^s_{d,h(t-\tau)k} - q^s_{htk} + r_{htk} - s^s_{htk} \right) \\ &\qquad \forall h, \forall t, \forall k \in [2, NK], \forall s \end{aligned} \tag{26}$$

$$\begin{aligned} v^s_{ht1} &= v^s_{h(t-1)NK} + \frac{1}{NK} \\ &\quad \cdot \left(RC_h \cdot q^s_{d,h(t-\tau)1} - q^s_{ht1} + r_{ht1} - s^s_{ht1} \right) \\ &\qquad \forall h, \forall t, \quad \forall s \end{aligned} \tag{27}$$

$$s^{\min}_h \le s^s_{htk} \le s^{\max}_h \tag{28}$$

$$\begin{aligned} &q^s_{d,h(t-\tau)k} \\ &\quad = \left[q^s_{1(t-\tau)k} \cdots q^s_{(h-1)(t-\tau)k} 0 q^s_{(h+1)(t-\tau)k} \cdots q^s_{NH(t-\tau)k} \right] \end{aligned} \tag{29}$$

In (18), the intrahour wind power in scenario s (P^s_{wtk}) is equal to the wind power forecast $(P^{f,s}_{wtk})$ minus the nonnegative curtailed wind power $(P^{c,s}_{wtk})$. The intrahour hydro power generation P^s_{htk} is dependent on the water discharge rate which is subject to the discharge limit (19). Ramping limits (20) show that the hydro power increment in two consecutive intrahours is limited. The wind-hydro coordination with sufficient ramping provides complimentary power from cascaded hydro units to wind units to make $P^s_{\Delta,wtk} = 0$ for all wind units in $S_{C,h}$. In (21) and (22), the hourly hydro unit commitment is related to startup and shutdown indicators.

The intrahour hydro power generation is dependent on water discharge in (23). The intrahour reservoir volume constraints of hydro units are given in (24) and (25). The intrahour reservoir volume in (26) is dependent on its previous intrahour value,

discharge water flow in the present intrahour, inflow water flow from upstream hydro unit, inflow water flow, and spillage in each intrahour. In (27), the volume in the first intrahour of each hour is dependent on the volume in the last intrahour of the previous hour, the present net water flow rate, spillage, inflow and inflow from upstream hydro units. The intrahour quantities in (28) and (29) are similar to (7) and (8).

C. Risk Assessment

A GENCO would be concerned with the risk associated with its payoff when considering market price uncertainties [17], [18]. Suppose the GENCO's day-ahead target payoff is T_0. The payoff risk given in (30) is associated with the failure to meet the target payoff. The linear expression of risk (30) is represented in (31) by auxiliary binary variables

$$R^s = \begin{cases} T_0 - PF^s, & \text{if } PF^s < T_0 \\ 0, & \text{otherwise} \end{cases} \tag{30}$$

$$0 \le R^s - [T_0 - PF^s] \le M \cdot [1 - \delta^s]$$

$$0 \le R^s \le M \cdot \delta^s. \tag{31}$$

Here, the expected downside risk is smaller than the accepted risk level. If a GENCO is not satisfied with its payoff that is below the target, an upper expected downside risk given in (32) will be appended into the PBUC formulation

$$\text{EDR} = E(R^s) = \sum_{s=1}^{\text{NS}} p^s \cdot R^s \le \overline{\text{EDR}}. \tag{32}$$

Hence, the original risk-neutral model is turned into a risk-constrained model by including (31)–(32). The objective is to calculate the expected payoff while keeping the expected downside risk within an acceptable range. The target $\overline{\text{EDR}}$ should be carefully designed since a tight constraint on the expected downside risk (i.e., relatively low risk $\overline{\text{EDR}}$ or high targeted payoff) could result in an infeasible solution.

D. Risk-Based Stochastic PBUC Solution

The proposed stochastic PBUC for the cascaded hydro and wind unit coordination is solved by a MIP package (CPLEX).

The deterministic PBUC solution is obtained when uncertain variables are replaced by their forecasts. If the transmission network is considered, the dimension of the stochastic PBUC can increase significantly. The solution techniques based on the Benders' decomposition are considered to deal with large-scale systems by decomposing the problem into tractable master UC and hourly network evaluation subproblems [29], [30].

III. Numerical Examples

In this section, two case studies are illustrated to investigate coordinated and uncoordinated scheduling strategies in the GENCO's portfolio with cascaded hydro and wind units. We assume no transmission congestion among wind and hydro units since they belong to the same GENCO. Detailed hydro unit data are given in Table I, where a, b, c are the quadratic, linear, and constant coefficients of water-to-power conversion curves, respectively. The errors in market price forecast (i.e., day-ahead MCPs and energy balancing price) and the wind energy forecast uncertainty are simulated via 10 000 scenarios using the Monte Carlo simulation, and efficient algorithms are used to reduce the number of scenarios [19], [20]. In the following, a three-hour ahead case and a day-ahead case are studied.

TABLE I
CHARACTERISTICS OF CASCADED HYDRO UNITS

Description	H1	H2	H3	H4	H5	H6	H7
$P_{\min,h}$ (MW)	9.0	4.0	17.0	30.0	9.0	2.0	19.0
$P_{\max,h}$ (MW)	70.0	70.0	115.0	194.0	80.0	60.0	120.0
RD_h (MW/min)	1.17	1.17	1.92	3.23	1.33	1.00	2.00
RU_h (MW/min)	1.17	1.17	1.92	3.23	1.33	1.00	2.00
a (MW/(Hm³/h)²)	-42	-30	-12.5	-31	-38.8	-31.2	-14.4
b (MW/(Hm³/h))	113	106.2	78.8	155.1	121.75	98.42	85.5
c (MW)	-1.82	-6.0	7.26	7.5	-2.64	-7.23	6.45
$q_{\min,h}$ (Hm³/h)	0.1	0.1	0.13	0.15	0.1	0.1	0.15
$q_{\max,h}$ (Hm³/h)	1.0	1.0	2.0	2.0	1.0	1.0	2.0
r_h (Hm³/h)	0.4	0.3	0.2	0.3	0.3	0.2	0.12
$s_{\min,h}$ (Hm³/h)	0.1	0.1	0.2	0.2	0.1	0.1	0.2
$s_{\max,h}$ (Hm³/h)	1.0	1.0	2.0	2.0	1.0	1.0	2.0
$V_{0,h}$ (Hm³)	10.0	8.0	17.0	11.0	10.0	9.0	18.0
$V_{NT,h}$ (Hm³)	10.0	8.0	17.0	11.0	10.0	9.0	18.0
$V_{\min,h}$ (Hm³)	7.0	4.0	10.0	7.0	6.0	5.0	12.0
$V_{\max,h}$ (Hm³)	15.0	13.0	24.0	16.0	16.0	14.0	30.0
Catchment Index	1	1	1	1	2	2	2
Upstream Unit	-	-	H2,H1	H3	-	H5	H6
Downstream Unit	H3	H3	H4	-	H6	H7	-
Delay Time	2	2	2	2	2	2	2

TABLE II
THREE-HOUR AHEAD CASES

Case	Coordinate	Stochastic	Energy Balancing Price ($/MWh)
1	No	No	5.00
2	No	Yes	5.00
3	No	No	50.00
4	No	Yes	50.00
5	Yes	No	-
6	Yes	Yes	-

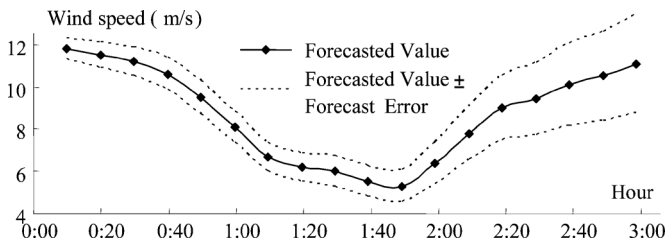

Fig. 1. Wind speed forecast.

A. Three-Hour Ahead Scheduling

Table I shows the system data in which a 3-h coordination of hydro unit H1 is considered with a 200-MW wind generating unit. Table II shows the six cases in which risk constraints are not included. The forecasts for wind and day-ahead MCP and their respective forecast errors are given in Figs. 1 and 2. Based on the available forecasting techniques, the wind speed forecast would have a larger error (i.e., 10%–20%) than the price forecast (less than 10%); thus a higher standard deviation is used to represent wind speed forecast errors.

The wind speed forecast follows the Weibull distribution function, with the Weibull constant equal to 2 and the average wind speed equal to 9.1 m/s. The 3-h pattern strength is 0.34 at the peak hour 3, which is the ratio of the peak wind speed to the average wind speed during the 3-h period. The ARMA model is

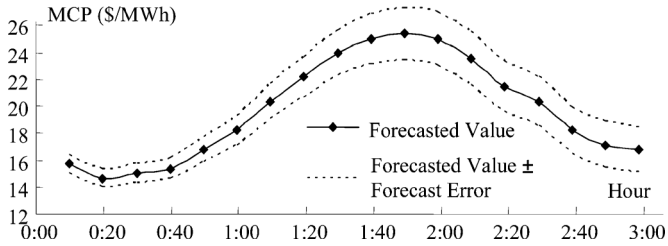

Fig. 2. Day-ahead MCP forecast.

used to simulate the wind speed forecast error [27], [28]. Since the autocorrelation factor (ACF) and partial autocorrelation factor (PACF) decrease dramatically as the time lag increases, a lower order ARMA (1,1) represented in (33) is used.

$$X(t,k) = \alpha \cdot X(t,k-1) + \beta \cdot Z(t,k-1) + Z(t,k) \quad k \in [2, NK]$$
$$X(t,1) = \alpha \cdot X(t-1,NK) + \beta \cdot Z(t-1,NK) + Z(t,1). \tag{33}$$

ARMA constants can be procured by minimizing the difference in the root mean square error (RMSE) between the simulated ARMA model and the wind speed measurement data [28]. In this paper, it is assumed that the ARMA constants are $\alpha = 0.88, \beta = -0.34$. The standard deviation represented by the truncated Gaussian distribution function $[-\sigma, +\sigma]$ in which σ ranges from 3% of the wind speed forecast for a 10-min lag time to 11% of the wind speed forecast for a 3-h lag time, which shows that the forecast error increases linearly in the forecast horizon. Once a large number of scenarios are generated, the boundary levels are derived by the maximum deviations of wind speed scenarios located above/below the forecast, as shown in Fig. 1.

Similarly, autoregressive integrated moving average (ARIMA) is used to procure the price forecast error, which is a nonstationary stochastic process. The nonstationary forecasted time series can be represented by periodic and stationary time series. In this case, the trend of periodic component is shown in Fig. 2, while the standard deviation of the stationary component represented by the truncated Gaussian distribution function $[-\sigma, +\sigma]$ is 1% for a 10-min lag and 5% for a 3-h lag [31]. The standard deviation of stationary components increases linearly with the time-lag. The 3-h pattern strength is 0.28, and the peak price hour is 1:50. The average price is 19$/MWh. The boundary levels in Fig. 2 show the maximum deviation of random variables located above/below the forecast at each time interval.

The number of scenarios is reduced to 3 with the corresponding probabilities of 0.5188, 0.1822, and 0.2990, respectively. The probabilities are procured by eliminating scenarios with very low probabilities and bundling scenarios that are very close in terms of statistical metrics [19], [20]. The simulation results are compared in coordinated and uncoordinated scheduling cases. The payoffs for Cases 1–6 are summarized in Table III with a target payoff of $6000. The results are discussed as follows.

TABLE III
PAYOFFS IN THE THREE-HOUR AHEAD PROBLEM ($)

	Case 1	Case 2	Case 3	Case 4	Case 5	Case 6
Imbalance Costs	1,395	1,598	3,055	933	0	0
Wind Energy Sales	6,153	6,280	4,354	4,348	4,529	4,713
Wind Energy Payoff	4,758	4,682	1,299	3,415	4,529	4,713
Hydro Energy Payoff	2,111	2,275	2,111	2,275	2,098	1,637
Total Payoff	6,869	6,957	3,410	5,690	6,627	6,350
EDR	45	19	2,584	348	230	0

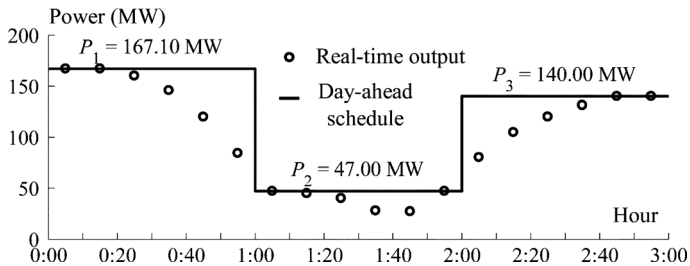

Fig. 3. Three-hour ahead schedule in Case 1.

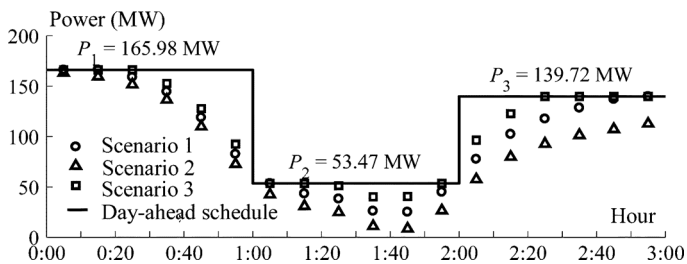

Fig. 4. Three-hour ahead schedule in Case 2.

1) Uncoordinated Scheduling of Wind and Hydro Units: Figs. 2–6 show the dispatch results for the uncoordinated scheduling Cases 1–4 listed in Table II. In Cases 1 and 2, the imbalance energy charges have a smaller impact on payoff since the energy balancing price is 5 $/MWh which is much lower than average MCPs.

We offer the following observations.

- *Deterministic versus stochastic scheduling solutions*

The imbalance energy, its cost, and the wind energy curtailment are higher in the stochastic solution. Figs. 3 and 4 show that there are 3.27 and 6.21 MWh of curtailments in Cases 1 and 2, respectively. Comparing Cases 3 and 4, the imbalance energy in Case 3 is 10.22 MWh while it increases to 13.13 MWh in Case 4. The imbalance energy charge in Case 3 is $711.55 which increases to $933.02 in Case 4. Figs. 5 and 6 show 59.98 and 63.30 MWh of curtailment in Cases 3 and 4, respectively. At certain intrahours, the wind power generation is not the same as its hourly dispatch which indicates that the wind power is curtailed to minimize imbalance energy charges. Table III shows that the stochastic scheduling solutions would lead to higher payoffs in the uncoordinated cases. The hydro unit payoff is also increased in the stochastic solutions; however, the wind unit payoff calculated by the energy balancing price increases from Cases 3 to 4, and decreases from Cases 1 to 2. The deterministic payoffs and imbalance energy costs in Table III are forecast values which are procured by applying deterministic values to uncertain parameters in the market.

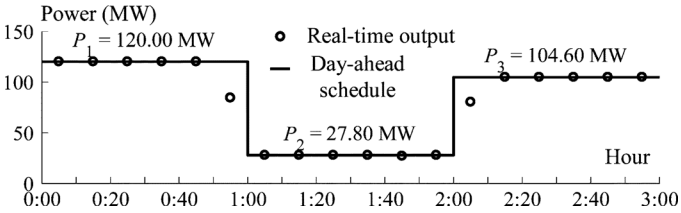

Fig. 5. Three-hour ahead schedule in Case 3.

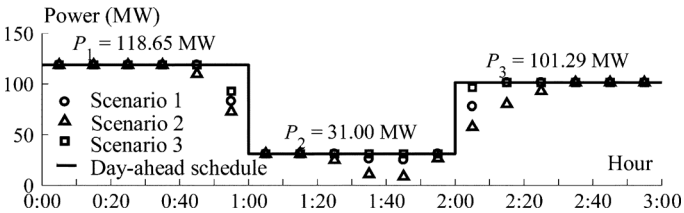

Fig. 6. Three-hour ahead schedule in Case 4.

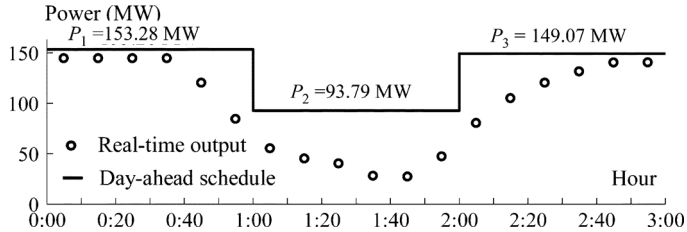

Fig. 7. Three-hour ahead schedule results in Case 5.

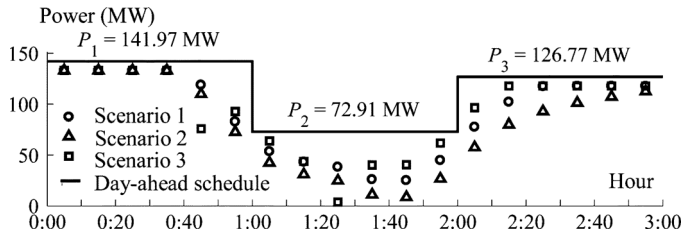

Fig. 8. Three-hour ahead schedule results in Case 6.

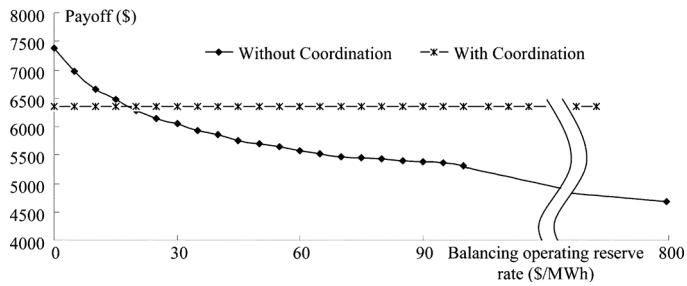

Fig. 9. Payoffs with energy balancing price.

- *Impact of energy balancing price on imbalance energy*

As the energy balancing price increases, the imbalance energy decreases. Here, the imbalance energy is decreased from 55.20 MWh in Case 1 to 10.22 MWh in Case 3. The same applies to Cases 2 and 4.

- *Impact of energy balancing price on wind energy curtailment*

Comparing Cases 1 and 2 with Cases 3 and 4, it is seen that higher energy balancing price increases the wind energy curtailment to avoid imbalance energy charges. The wind energy curtailment increases from 3.27 MWh in Case 1 to 59.98 MWh in Case 3. A similar observation can be procured for stochastic Cases 2 and 4.

- *Impact of energy balancing price on total payoff*

Table III shows a lower payoff when the energy balancing price is higher. A lower payoff occurs when the wind energy unit payoff is lowered due to the imposed energy balancing price. The comparison shows that the stochastic scheduling solution demonstrates a higher payoff once energy balancing prices are higher. The increase in payoff from Case 1 to Case 2 is 1.3% while the increase in payoff from Case 3 to Case 4 is 66.8%.

- *EDR in deterministic and stochastic cases*

The EDR of the deterministic solution measures the risk of the deterministic solution in terms of scenarios. The EDR for a target payoff of \$6000 is \$45.62 for the deterministic solution (Case 1) and \$19.50 for the stochastic solution (Case 2). The difference of \$26.12 shows a lower risk for the stochastic scheduling solution. Thus, the stochastic solution would increase the total payoff and decrease the financial risks as compared with the deterministic scheduling solution.

2) Coordinated Wind and Cascaded Hydro Units: Cases 5 and 6 investigate the benefits of coordinated dispatch of cascaded hydro and wind units. In comparison with Cases 1–4, imbalance energy charges are not incurred in Cases 5 and 6 since the scheduling coordination of wind and cascaded hydro units will firm up the output and $P^s_{\Delta,wtk}$ is zero. The following observations are deducted by comparing coordinated and uncoordinated scheduling cases.

- *Impact of stochastic analysis*

Figs. 7 and 8 show a wind energy curtailment of 12.42 and 37.08 MWh in Cases 5 and 6. Again, the wind energy curtailment is higher in the stochastic scheduling cases.

- *Impact on the total payoff and risk*

The coordinated Cases 5 and 6 in Table III show that the stochastic solution would result in lower risks and total payoffs. In Table III, although the downside risk is decreased in the stochastic solution, the total payoff is decreased by 4.2%. In addition, the cascaded hydro unit payoffs are decreased in the coordinated scheduling cases. Hence, the scheduling coordination may not be economically beneficial for cascaded hydro units. Comparing Cases 4 and 6, it is shown that higher energy balancing prices will lower the risk and increase the expected payoff with the coordination. However, Cases 2 and 6 show that the coordination may not improve the GENCO's expected payoff in a lower energy balancing price.

Fig. 9 presents the payoffs in Cases 4 and 6. For the uncoordinated Case 4, the expected payoff decreases with an increase in energy balancing price until the price is high enough to eliminate wind power deviations, so the payoff is the highest at the zero energy balancing price. In this case, the maximum expected payoff is \$7374.06 at $\rho_{BP} = 0$ \$/MWh, and the minimum payoff is \$4619.51 starting roughly at $\rho_{BP} = 800$ \$/MWh. In the coordinated Case 6, the expected payoff is constant since the energy balancing prices have no impact on payoffs. The uncoordinated and coordinated scheduling cases are equally profitable

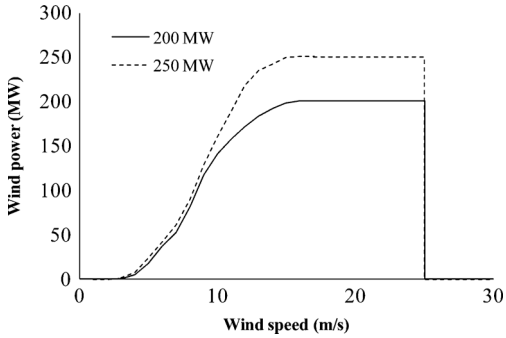

Fig. 10. Wind turbine power curves.

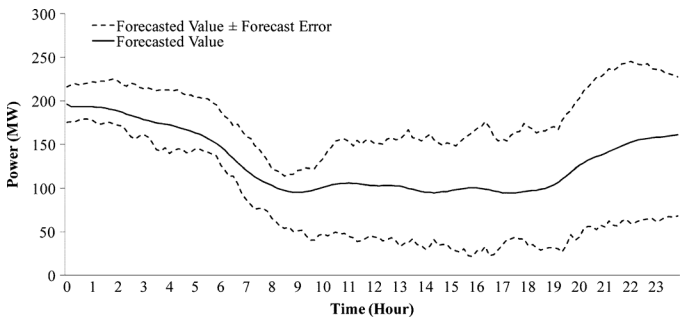

Fig. 11. Wind power forecast error of W3.

in Fig. 9 where the two curves cross ($\rho_{BP} = 18.2$ \$/MWh). Thus, the coordination provides a higher return when the energy balancing price is higher than 18.2 \$/MWh.

B. Day-Ahead Scheduling

We consider the day-ahead schedule in a GENCO with three wind farms (W1–W3) and seven hydro units in two catchments (H1–H4 in catchment 1 and H5–H7 in catchment 2). The wind farm capacities are 200, 200, and 250 MW, respectively and the wind power curves are shown in Fig. 10. We assume W1 and W2 are located near catchment 1 and W3 is close to catchment 2. Thus, the coordinated scheduling of W1–H2, W2–H3, and W3–H6 is considered.

The hydro unit characteristics are given in Table I, and market prices and wind speeds are forecasted as discussed before. Ten thousand scenarios are generated originally and 30 are retained after scenario reduction. In this case study, the standard deviation of forecast error of wind speeds increases linearly from 3% of forecasted wind speed for the 1-h lag time to 11% of forecasted wind speed for the 24-h lag time. The diurnal strength pattern is 0.34 with the average wind speed 9.1 m/s and hour of peak wind speed of 24. The wind generation forecast error of W3 is shown in Fig. 11. Here, the wind power forecast error is higher than that of the wind speed because of nonlinear and nonconvex characteristics of the wind turbine power curve. Alternatively, the forecast error of wind generation can be simulated by fat tailed Beta distribution function in which the parameters are dependent on wind generation levels [32].

The wind generation forecast error is procured based on the wind speed forecast error and four cases are studied, as shown in Table IV. The energy balancing price of 30\$/MWh is used in all four cases and risk constraint is imposed as given in Table IV.

TABLE IV
CASES CONSIDERED IN THE DAY-AHEAD SCHEDULING

Case	Coordination	W1	W2	W3	Stochastic	Risk-Constrained
1	No	-	-	-	Yes	No
2	No	-	-	-	Yes	Yes
3	Yes	H2	H3	H6	Yes	No
4	Yes	H2	H3	H6	Yes	Yes

TABLE V
UC FOR H2, H5 AND H6 IN CASE 1

Unit	Hours (1-24)																							
H2	0	0	0	0	1	0	0	1	1	1	1	1	1	1	1	1	1	1	1	1	1	0	0	0
H5	1	1	1	0	1	1	1	1	1	1	1	1	1	1	1	1	1	1	1	1	1	1	0	0
H6	0	1	1	0	1	0	1	1	1	1	1	1	1	1	1	1	1	1	1	1	1	1	0	0

TABLE VI
UC FOR H2, H5 AND H6 IN CASE 2

Unit	Hours (1-24)																							
H2	0	0	0	0	**0**	0	0	1	1	1	1	1	1	1	1	1	1	1	1	1	**1**	0	0	
H5	1	1	1	0	1	1	1	1	1	1	1	1	1	1	1	1	1	1	1	1	1	1	0	0
H6	**1**	1	1	0	1	0	1	1	1	1	1	1	1	1	1	1	1	1	1	1	1	1	0	0

TABLE VII
UC FOR H2, H5 AND H6 IN CASE 3

Unit	Hours (1-24)																							
H2	**1**	**1**	**1**	**1**	1	**1**	**1**	1	1	1	1	1	1	1	1	1	1	1	1	1	**1**	**1**	**1**	
H5	1	1	1	0	1	1	1	1	1	1	1	1	1	1	1	1	1	1	1	1	1	1	0	0
H6	**1**	1	1	**1**	1	**1**	1	1	1	1	1	1	1	1	1	1	1	1	1	1	1	**1**	**1**	

TABLE VIII
UC FOR H2, H5 AND H6 IN CASE 4

Unit	Hours (1-24)																							
H2	**1**	**1**	**1**	**1**	1	**1**	**1**	1	1	1	1	1	1	1	1	1	1	1	1	1	**1**	**1**	**1**	
H5	1	**0**	1	**1**	1	1	1	1	1	1	1	1	1	1	1	1	1	1	1	1	1	1	0	0
H6	**1**	1	1	**1**	1	**1**	1	1	1	1	1	1	1	1	1	1	1	1	1	1	1	**1**	**1**	

The stochastic PBUC has 160 010 continuous variables, 18 576 binary variables, and 171 685 constraints, which is solved in about 30 s with an Intel 2.13-GHz personal computer. The impact of coordination and risk constraints are evaluated on the GENCO's hourly scheduling, generation dispatch, and payoff. The results are discussed as follows.

- *Impact on Unit Commitment (UC)*

Tables V–VIII show the UC results for units H2, H5, and H6 in Cases 1–4. Comparing Cases 2–4 with Case 1, the hourly unit commitment changes are highlighted in Tables VI–VIII. The changes in Table VI are due to the inclusion of risk constraint. The UC solutions for units H2 and H6 are changed to satisfy the $\overline{\text{EDR}}$ limit for the given target payoff at the cost of lowering the payoff. The changes listed in Table VII are due to coordination. Similar to Case 2, the changes listed in Table VIII are due to risk constraints and coordination in Case 4. Since H5 is located on the upstream of H6 with a water discharge flow delay time of 2 h, the scheduling coordination of W3-H6 when considering the risk constraint would require the commitment of H5 at hour 4 as opposed to hour 2. H5 is shutdown at the end of the day to satisfy terminal reservoir requirements. In Case 4, H2 and H6 are committed at all hours for coordination with wind units.

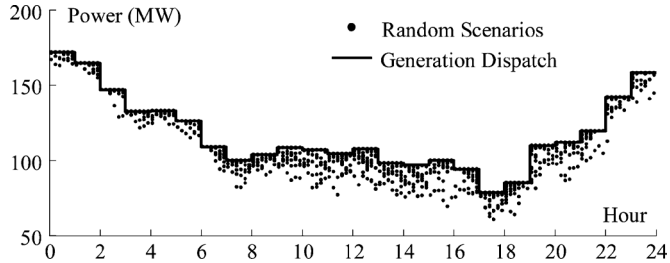

Fig. 12. Day-ahead generation dispatch of W1 in Case 1.

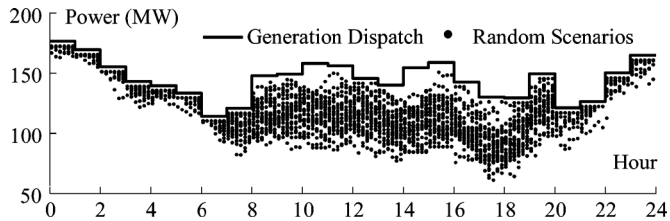

Fig. 13. Day-ahead generation dispatch of W1 in Case 3.

TABLE IX
EXPECTED PAYOFF AND DOWNSIDE RISK FOR ALL CASES ($)

Case	Expected Payoff	Downside Risk
1	897,956	7,648
2	897,498	7,000
3	914,083	3,082
4	913,756	3,000

- *Impact on generation dispatch*

Figs. 12 and 13 show the generation dispatch of W1 in Cases 1 and 3. The generation dispatch of W1 in Cases 2 and 4 have similar trends and thus are not presented here. As expected, the generation dispatch follows the trend in wind energy scenarios. Without any coordination, the optimal generation dispatch incurs an average wind power curtailment of 12.99 MW. The expected wind energy imbalance is 27.58 MWh for W1. With coordination, the average wind power curtailment is 3 MW which is 76.9% lower than that without coordination. The hydro unit generation is represented by the distance between dots and the generation dispatch curve. There is no imbalance wind energy because hydro units provide intrahour power to complement the wind unit generation.

- *Impact on payoff*

Table IX shows expected payoffs and downside risks with a target payoff of $900 000. If the expected downside risk of $7648 in Case 1 is unacceptable, the GENCO can control the associated risk level with the proposed method. In order to obtain the minimum allowable downside risk, the risk will be penalized in the objective function with a large penalty factor. Accordingly, the minimum downside risk is $6855 with an expected payoff of $896 730. In Case 2, an acceptable risk level is $7000 with a payoff of $897 498. In comparison with Case 1, the risk is reduced by $(7648–7000)/7648 = 8.48\%$ at the cost of reducing the expected payoff by $(\$897\,956–\$897\,498)/897\,956 = 0.05\%$.

In Case 3, EDR is $3082 with an expected payoff of $914 083. The minimum EDR is $2997 with an expected payoff of $913 747 which is procured by penalizing the risk into the objective. In Case 4, we set the maximum EDR to $3000 and obtain an expected payoff of $913 756, which shows a reduction in risk of 2.66% at the cost of 0.04% reduction in payoff, as compared to Case 3.

Table IX shows that the scheduling coordination will increase the expected payoff and decrease the downside risk. By setting EDR in an acceptable range in Cases 2 and 4, the expected payoff in the coordinated Case 4 will be higher. Table IX shows that the acceptable EDR in Case 4 is far less than that in Case 2; hence scheduling coordination will decrease EDR and increase the expected payoff.

IV. CONCLUSION

The proposed study and its results demonstrate that the scheduling coordination of cascaded hydro and wind units can firm up wind energy, increase expected payoffs, and reduce downside risks of GENCOs. When wind and hydro units are not coordinated, energy balancing prices would affect the generation dispatch decisions. Also, the expected payoff will decrease when the energy balancing price is increased. It is shown that depending on the energy balancing price, the payoff in uncoordinated hydro and wind unit cases may be larger than that in coordinated cases. Hence, the GENCO may decide to schedule cascaded hydro and wind units in either coordinated or uncoordinated configurations, which depends on the accuracy of forecast of the day-ahead energy balancing price. The wind energy curtailment will increase with energy balancing prices, in order to avoid imbalance energy charges. Thus, the coordination of wind and hydro scheduling would lower the wind curtailment and increase the GENCO's payoff by mitigating the imbalance energy charges. The coordination will result in lower wind curtailment in both stochastic and deterministic scheduling solutions. It is shown that the hydro unit payoffs will decrease once they are coordinated with wind energy units. However, eliminating the imbalance energy charges for wind energy units in coordinated cases could increase the total payoff of a GENCO at certain energy balancing prices.

The stochastic scheduling solution would lower the GENCO's expected downside risk as compared to the deterministic scheduling solution. In addition, in uncoordinated cases, the stochastic scheduling solution will result in higher payoffs for a GENCO as compared to the deterministic scheduling solution.

Other storage technologies, such as the vanadium redox-flow battery (VRB) storage and pumped-storage hydro, may also be used to firm up wind energy. However, storage efficiency cycle, storage capacity, reservoir balance, and limited number of charge/discharge cycles per day could increase wind power curtailments and limit the GENCO's payoffs.

REFERENCES

[1] A. Pullen and M. Eneland, Global Wind 2006 Report GWEC, Global Wind Energy Council, Brussels, Belgium, May 2007 [Online]. Available: http://www.gwec.net/index.php?id=78

[2] International Energy Agency, Variability of Wind Power and Other Renewables-Management Options and Strategies June 2005 [Online]. Available: http://www.awea.org/policy/regulatory_policy/transmission_documents/iea_report_variability_wind.pdf

[3] P. B. Eriksen, T. Ackermann, H. Abildgaard, P. Smith, W. Winter, and J. R. Garcia, "System operation with high wind penetration," *IEEE Power Energy Mag.*, vol. 3, no. 6, pp. 65–74, Nov./Dec. 2005.
[4] M. Ahlstrom, L. Jones, R. Zavadil, and W. Grant, "The future of wind forecasting and utility operations," *IEEE Power Energy Mag.*, vol. 3, no. 6, pp. 57–64, Nov./Dec. 2005.
[5] G. Kariniotakis *et al.*, "Next generation forecasting tools for the optimal management of wind generation," in *Proc. Int. Conf. Probabilistic Methods Applied to Power Systems*, Jun. 2006, pp. 1–6.
[6] I. Sánchez, "Short-term prediction of wind energy production," *Int. J. Forecast.*, vol. 22, no. 1, pp. 43–56, Jan. 2006.
[7] "ERCOT wind impact/integration analysis, phase 1 review: Variability and predictability," in *Proc. ROS Wind A/S Task Force Meeting*, Oct. 2007 [Online]. Available: http://www.ercot.com/meetings/ros/keydocs/2007/1022/Variablity_and_Predictability_draft_dlvd_2a.zip
[8] "ERCOT wind impact/integration analysis, phase 2 review: Ancillary services requirements," in *Proc. Wind Impact Task Force Meeting*, Feb. 2008 [Online]. Available: http://www.ercot.com/meetings/ros/keydocs/2008/0201/ERCOT_AS-Ph2_d7.pdf
[9] T. Hennessy and M. Kuntz, "The multiple benefits of integrating electricity storage with wind energy," in *Proc. 2005 IEEE Power Engineering Society General Meeting*, Jun. 2005, vol. 2, pp. 1952–1954.
[10] J. C. Smith, M. Milligan, E. A. DeMeo, and B. Parsons, "Utility wind integration and operating impact state of the art," *IEEE Trans. Power Syst.*, vol. 22, no. 3, pp. 900–908, Aug. 2007.
[11] J. Wang, M. Shahidehpour, and Z. Li, "Security-constrained unit commitment with volatile wind power generation," *IEEE Trans. Power Syst.*, vol. 23, no. 3, pp. 1319–1327, Aug. 2008.
[12] A. Tuohy, P. Meibom, E. Denny, and M. O'Malley, "Unit commitment for systems with significant wind penetration," *IEEE Trans. Power Syst.*, vol. 24, no. 2, pp. 592–601, May 2009.
[13] R. Billinton, B. Karki, R. Karki, and G. Ramakrishna, "Unit commitment risk analysis of wind integrated power systems," *IEEE Trans. Power Syst.*, vol. 24, no. 2, pp. 930–939, May 2009.
[14] M. Shahidehpour, H. Yamin, and Z. Li, *Market Operations in Electric Power Systems*. Hoboken, NJ: Wiley, 2002.
[15] T. Li and M. Shahidehpour, "Strategic bidding of transmission-constrained GENCOs with incomplete information," *IEEE Trans. Power Syst.*, vol. 20, no. 1, pp. 437–447, Feb. 2005.
[16] J. M. Arroyo and A. J. Conejo, "Optimal response of a power generator to energy, AGC, and reserve pool-based markets," *IEEE Trans. Power Syst.*, vol. 17, no. 2, pp. 404–410, May 2002.
[17] T. Li and M. Shahidehpour, "Risk-constrained bidding strategy with stochastic unit commitment," *IEEE Trans. Power Syst.*, vol. 22, no. 1, pp. 449–458, Feb. 2007.
[18] L. Wu, M. Shahidehpour, and Z. Li, "GENCO's risk-constrained hydrothermal scheduling," *IEEE Trans. Power Syst.*, vol. 23, no. 4, pp. 1847–1858, Nov. 2008.
[19] J. Dupacová, N. Gröwe-Kuska, and W. Römisch, "Scenario reduction in stochastic programming: An approach using probability metrics," *Math. Program.*, ser. A 95, pp. 493–511, 2003.
[20] GAMS/SCENRED Documentation [Online]. Available: http://www.gams.com/docs/document.htm
[21] 2006 State of the Market Report: Volume II PJM Interconnection, Market Monitoring Unit, Mar. 2007, pp. 151–158 [Online]. Available: http://www2.pjm.com/markets/market-monitor/downloads/mmu-reports/2006-som-volume-ii.pdf
[22] S. Mariano, M. Calado, and L. Ferreira, "Dispatch of head dependent hydro units: Modeling of optimal generation in electricity market," in *Proc. IEEE Power Tech.*, Bucharest, Jun. 2009, pp. 1–6.
[23] S. Bisanovic, M. Hajro, and M. Dlakic, "Hydrothermal self-scheduling problem in a day-ahead electricity market," *Elect. Power Syst. Res.*, vol. 78, no. 9, pp. 1579–1596, Sep. 2008.
[24] X. Guan, E. Ni, R. Li, and P. B. Lu, "An optimization-based algorithm for scheduling hydrothermal power systems with cascaded reservoirs and discrete hydro constraints," *IEEE Trans. Power Syst.*, vol. 12, no. 4, pp. 1775–1780, Nov. 1997.
[25] T. Li and M. Shahidehpour, "Price-based unit commitment: A case of Lagrangian relaxation versus mixed integer programming," *IEEE Trans. Power Syst.*, vol. 20, no. 4, pp. 2015–2025, Nov. 2005.
[26] J. F. Manwell *et al.*, Hybrid2—A hybrid system simulation model theory manual Renewable Energy Research Laboratory, Department of Mechanical Engineering, University of Massachusetts, Jun. 2006.
[27] L. Söder, "Simulation of wind speed forecast errors for operation planning of multiarea power systems," in *Proc. 2004 Int. Conf. Proc. Probabilistic Methods Applied to Power Systems*, Sep. 12–16, 2004, pp. 723–728.
[28] A. Boone, "Simulation of Short-Term Wind Speed Forecast Errors Using a Multi-Variate ARMA (1,1) Time-Series Model," Master Thesis, KTH, Stockholm, Sweden, 2005.
[29] M. Shahidehpour and Y. Fu, "Benders decomposition—Applying Benders decomposition to power systems," *IEEE Power Energy Mag.*, vol. 3, no. 2, pp. 20–21, Mar. 2005.
[30] L. Wu and M. Shahidehpour, "Accelerating the Benders decomposition for network-constrained unit commitment problems," *Energy Syst.*, vol. 1, no. 3, pp. 339–376, Jul. 2010.
[31] M. Zhou, Z. Yan, and G. Li, "An ARIMA approach to forecasting electricity price with accuracy improvement by predicted errors," in *Proc. IEEE Power Engineering Society General Meeting*, Jun. 2004, vol. 1, pp. 233–238.
[32] H. Bludzuweit, J. A. Dominguez-Navarro, and A. Llombart, "Statistical analysis of wind power forecast error," *IEEE Trans. Power Syst.*, vol. 23, pp. 983–991, Aug. 2008.

Lisias V. L. Abreu (M'05) received the Ph.D. degree in electrical engineering from Illinois Institute of Technology in 2008.

His research interests include renewable energies, electricity markets, and power system operation and control.

Mohammad E. Khodayar (S'09) received the B.S. and M.S. degree in electrical engineering from Amirkabir University of Technology (Tehran Polytechnic) and Sharif University of Technology, respectively. Presently he is working toward the Ph.D. degree in electrical engineering at Illinois Institute of Technology, Chicago, IL.

His research interests include renewable energies, electricity markets, and power system operation and control.

Mohammad Shahidehpour (F'01) is the Bodine Professor and Director of the Robert W. Galvin Center for Electricity Innovation, Illinois Institute of Technology, Chicago, IL.

Dr. Shahidehpour is the recipient of the 2009 Honorary Doctorate for the Polytechnic University of Bucharest in Romania. He is a Research Professor at the King Abdulaziz University in Saudi Arabia and Honorary Professor at Sharif University of Technology in Iran and North China Electric Power University in China. He is an IEEE Distinguished Lecturer.

Lei Wu (M'07) received the B.S. degree in electrical engineering and the M.S. degree in systems engineering from Xi'an Jiaotong University, China, in 2001 and 2004, respectively, and the Ph.D. degree in electrical engineering from Illinois Institute of Technology, Chicago, IL, in 2008.

He was a Senior Research Associate in the Electrical and Computer Engineering Department at Illinois Institute of Technology from 2008 to 2010. Presently, he is an Assistant Professor in the Electrical and Computer Engineering Department at Clarkson University, Potsdam, NY. His research interests include power systems restructuring and reliability.